Chapter 6

Lattice Design

This chapter discusses the lattice design of KEKB in detail. Specific requirements to consider are the following:

1. Realize the beam parameters listed in Table 2.2.
2. Ensure a sufficiently large dynamic aperture for a high injection efficiency and a long beam lifetime, particularly the Touschek lifetime in the LER.
3. Maintain a wide range of tunability for the beam parameters, especially for the horizontal emittance.
4. Allow a reasonable amount of tolerance for machine errors.

Because of the small β_y^* ($\sim$ 1 cm) at the interaction point (IP), a large amount of chromaticity is produced, and it has to be corrected without sacrificing the dynamic aperture. Discussions on the dynamic aperture and the sources that cause its reduction are given in section 6.1. The development of the ring lattice design is presented in section 6.2. Designs of the straight section beam optics are given in sections 6.3 and 6.4. Sections 6.5 and 6.6 examine the required magnet field qualities and tolerances.

6.1 Dynamic Aperture

For efficient beam injection at KEKB it is considered that the lattice design should allow a momentum aperture of at least $\pm 0.5\%$ and a transverse aperture of $> 1.2 \times 10^{-5}$ m. For maintaining a sufficiently long beam lifetime ($\sim$ 10 hours or better in the absence of machine errors), an even larger aperture is strongly favored.

A major cause for the reduction of the transverse dynamic aperture is the nonlinearity of sextupole magnets which are introduced to correct the chromaticity in the

ring. To solve this problem, it is considered best to use a pair of identical sextupole magnets that are connected with a $-I$ transformer in both the horizontal and vertical planes. This allows to cancel transverse nonlinearity of the sextupole magnets to the third order in the Hamiltonian[1]. Then, residual terms come to limit the dynamic aperture. In the case of KEKB, the vertical dynamic aperture is limited by: (1) the kinematic term of the drift space around the IP, and (2) the fringe field of the final quadrupole magnets at the edge, facing the IP[2].

A source of momentum aperture limitation is the modulation of linear betatron oscillations due to the synchrotron motion. If the beta functions at cavities have dependencies on the momentum, a change of the momentum by the cavity RF field produces a mismatch between the beam and the betatron phase space ellipse. This excites synchrotron-betatron resonances at $2\nu_{x,y} \pm m\nu_s = N$, and an exponential growth of transverse betatron amplitudes results. The momentum aperture is significantly degraded near these resonances. Resonances of smaller orders are more harmful. To avoid this problem a small synchrotron tune is required, such that those resonance conditions are not met[2]. The chromaticity in the x-y coupling terms is another source that limits the momentum aperture, since the compensation of the detector solenoid at the IP is not perfect, as described below.

As mentioned in the previous chapter, a small momentum compaction factor is needed to reduce the synchrotron tune, while keeping the bunch length and the momentum spread constant. When the linear momentum compaction is made small, the effects of higher-order momentum compaction becomes non-negligible. For example, the second order term produces an imbalance of the dynamic aperture for the positive and negative sides of the momentum deviation of a particle. This is due to eccentric motions of particles in the longitudinal phase space induced by the second-order momentum compaction.

Yet one more source of aperture limitation is the chromo-geometric aberration caused by a breakdown of the $-I$ transformer for off-momentum particles. This aberration becomes serious in the sextupole pairs for the local chromaticity correction scheme in the LER, which is discussed in Section 6.2.5. This problem arises, because the product of the sextupole strength and the vertical beta function at the sextupole magnets becomes much larger than in the arcs.

For a given lattice layout, the excitations of sextupole magnets are determined by evaluating the off-momentum optics directly, *i.e.* not by using perturbative methods. The solution of the sextupole excitations is calculated so as to simultaneously minimize the deviations of the betatron tune $\nu_{x,y}$ and Twiss parameters $\beta^{RF}_{x,y}$ and $\alpha^{RF}_{x,y}$ for a few points in the RF section. The momentum bandwidth considered is 1.5% for the HER

and $2 \sim 3\%$ for the LER. The number of fitting points of the momentum bandwidth is typically 20. All of the sextupole pairs are treated independently. (The results of the chromaticity correction are shown in Figures 6.5 and 6.6.) Optimization can be improved by matching for finite betatron amplitudes or by a nonlinear optimization of the dynamic aperture itself.

The dynamic aperture is estimated by tracking particles in six-dimensional phase space $(x, p_x, y, p_y, z, \delta)$ using SAD. Here, the variable z is defined as $z = -vt$, where t is the delay from the nominal particle. SAD is a fully symplectic tracking code, developed at KEK. It incorporates all known terms, such as linear and nonlinear fringe fields, thick lens multipole fields, kinematic terms, overlap of the solenoid field and other magnets, etc. In this study, the initial conditions are given as $p_{x0} = p_{y0} = z_0 = 0$ and $y_0 = ax_0$, where a is a constant. The dynamic aperture is expressed by the initial values of the action $2J_{x,y0}$ and the momentum deviation δ_0 of the particles which survived 1000 turns without damping due to synchrotron radiation. Although this period, which corresponds to 1000 turns, is only 1/8 of the transverse damping time of the LER, the results of 1000-turn tracking are almost equal to, or slightly smaller than, those of 8000-turn with radiation damping. Therefore, 1000-turn tracking is considered to be a sufficiently accurate estimation of the dynamic aperture.

The dynamic aperture is evaluated in two ways:

1. With the initial condition $y_0 = x_0/3$. This is to check the acceptance for horizontal beam injection.

2. With the initial condition $y_0 = x_0/\sqrt{50}$. This is for estimating the Touschek lifetime at collision with an emittance ratio of 2%. The Touschek lifetime is evaluated while assuming that the dynamic aperture in the J_x-J_z plane is given by $0 \leq (J_x/J_x^{\max}) + (J_z/J_z^{\max}) \leq 1$. See Figures 6.8 and 6.10 for illustrations of this approximation.

6.2 Development of Beam Optics Design

We have so far studied five types of optics design, as listed in Table 6.1. These optics have different combinations of cell structures and chromaticity correction schemes. All of the optics have been designed to give the required values of the horizontal emittance and the momentum spread. We have compared the performance of these optics in light of the following requirements:

1. To give a small synchrotron tune, and

2. To have a sufficiently large dynamic aperture for beam injection and for the Touschek lifetime.

The results are summarized in Table 6.1 and Figure 6.1. In the following subsections these designs are reviewed one by one. Since the second criterion above is especially challenging for the LER, we will discuss mainly issues concerning the LER.

	Injection	Touschek	ν_s
Interleaved $\pi/3$ FODO Cell	bad	bad	bad
Noninterleaved $\pi/2$ FODO Cell	good	fair	bad
Noninterleaved π Cell	excellent	fair	good
Noninterleaved 2.5π Cell	excellent	good	excellent
Noninterleaved 2.5π Cell +Local Chromaticity Correction	excellent	excellent	excellent

Table 6.1: Comparison of the performances of the cell structures and chromaticity correction schemes for the LER.

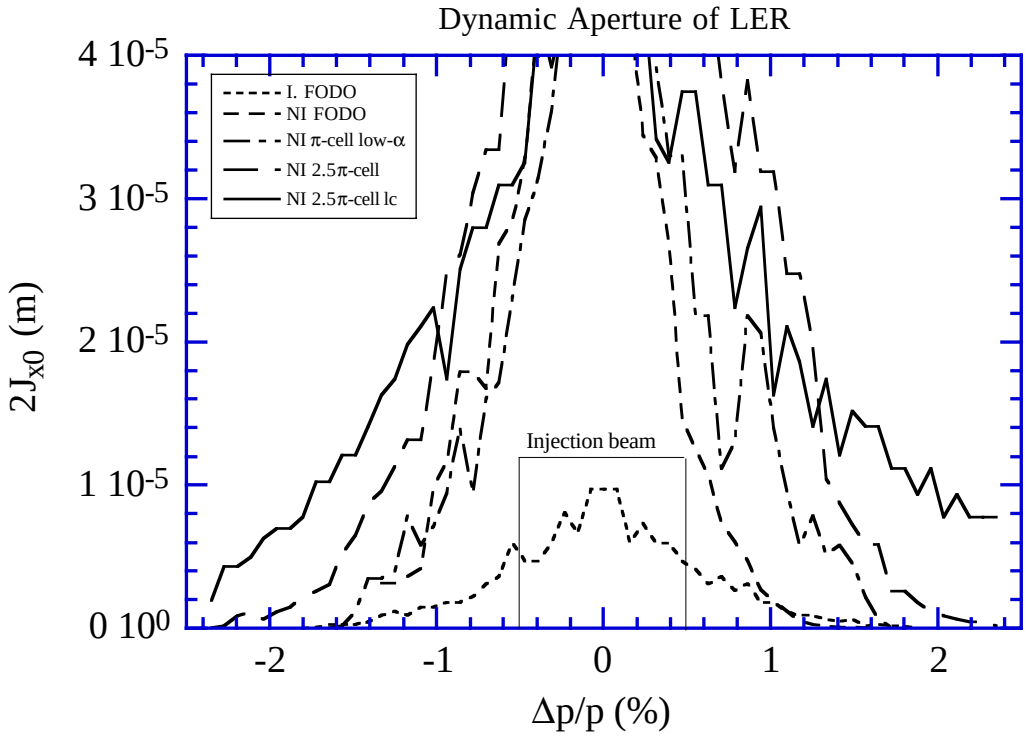

Figure 6.1: Dynamic aperture of the LER with five types of beam optics.

6.2.1 Interleaved $\pi/3$ FODO Cell

We have tried a conventional chromaticity correction scheme with interleaved sextupole magnets in $\pi/3$ FODO cells, where each quadrupole magnet is associated with a sextupole magnet. Sextupole magnets that are separated by the π phase difference are paired so as to cancel the lowest order of the transverse nonlinearity. We have tried chromaticity corrections with 6, 12, and 24 sextupole families. In all cases, the dynamic aperture remained too small, and did not satisfy the requirement. This interleaved sextupole scheme has been abandoned.

6.2.2 Noninterleaved $\pi/2$ FODO Cell

An arc lattice based on $\pi/2$ FODO cells with a chromaticity correction scheme with noninterleaved sextupole magnets has been considered. As the first step, the bend radius ρ is determined based on the requirement for the momentum spread. In electron storage rings with a constant bending radius and smooth focusing, the horizontal emittance ε_x and the momentum compaction factor α_p are given by

$$\varepsilon_x = 2\sigma_\delta^2 \langle H \rangle_{\text{bend}} \approx \frac{2R_A\sigma_\delta^2}{\nu_x^3}, \tag{6.1}$$

$$\alpha_p = \frac{2\pi}{C} \langle \eta_x \rangle_{\text{bend}} \approx \frac{2\pi R_A}{C\nu_x^2}. \tag{6.2}$$

Here, R_A is the average radius of the arc, ν_x the total horizontal tune of the arc, η_x the horizontal dispersion, and $H = \beta_x \left(\eta_x' + \alpha_x\eta_x/\beta_x\right)^2 + \eta_x^2/\beta_x$. The symbol $\langle f \rangle_{bend}$ represents the average of a quantity f in bend magnets.

According to Equations 6.1 and 6.2, once ρ is fixed, ε_x and α_p are uniquely determined by the total tune ν_x. Thus, if the arc is built with FODO cells to give $\varepsilon_x = 1.8 \times 10^{-8}$m, the momentum compaction factor becomes too big. This, in turn, means that $\nu_s \geq 0.06$, and produces serious difficulties in finding adequate operating points in the tune space. The anomalous emittance due to chromaticity can also become very large when ν_s is high [3]. In addition, the accelerating voltage becomes excessively high, if the short bunch length required in the design is to be achieved. Because of these difficulties, this scheme has been rejected.

6.2.3 Noninterleaved π Cell

To obtain small momentum compaction α_p, we must reduce $\langle \eta_x \rangle_{bend}$, while keeping $\langle H \rangle_{bend}$ constant. This can be done by combining two $\pi/2$ FODO cells, where four bend magnets are merged into two, as shown in Figure 6.2. In this scheme, in addition

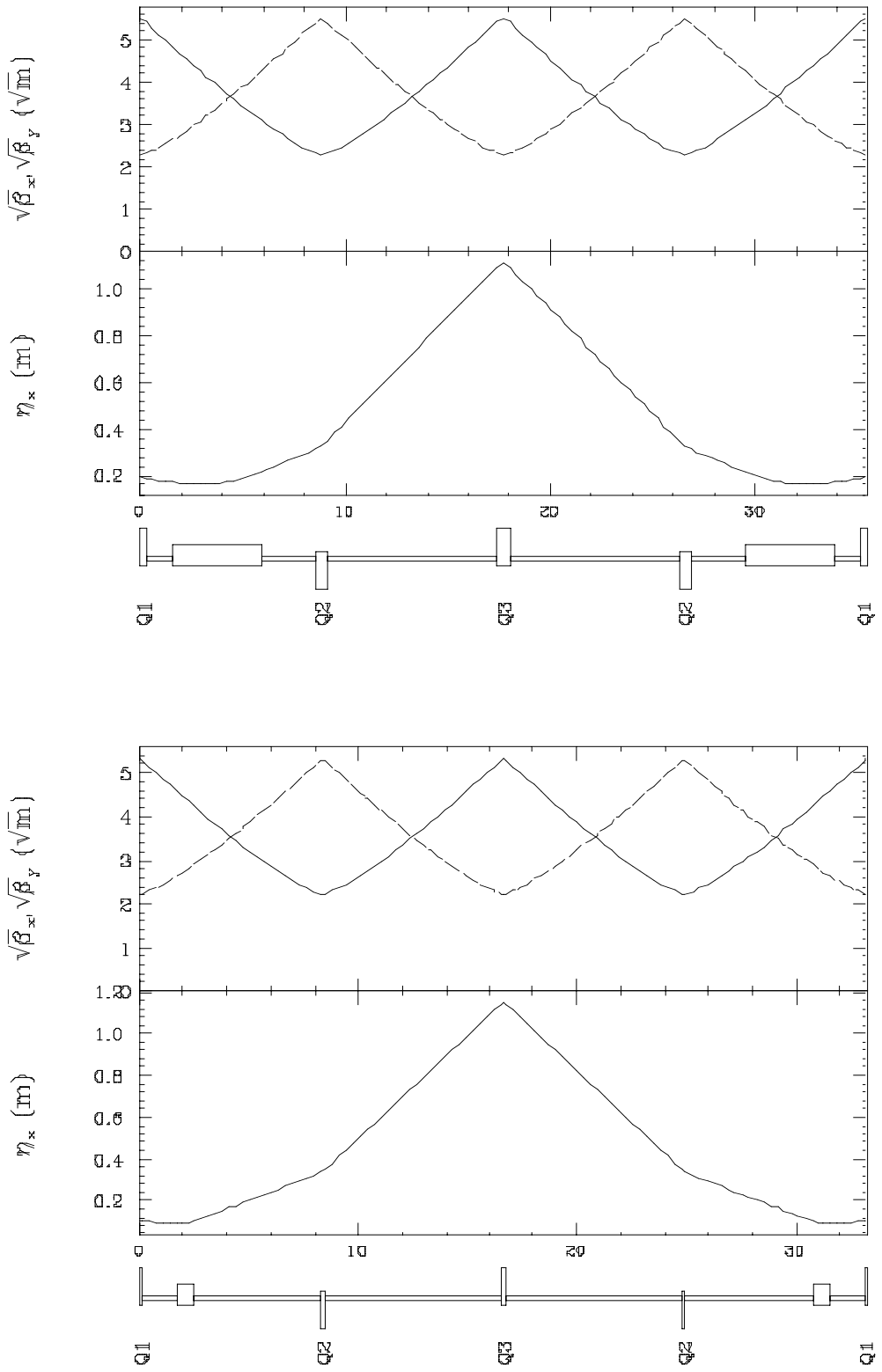

Figure 6.2: Structure of the π cell for the HER (above) and the LER (below).

to the total tune ν_x, the position of the bend magnets can also be taken as a free parameter for achieving the desired α_p and ε_x simultaneously. An acceptable solution was found for the LER. In the HER, since the bend magnets are longer than those in the LER, the variable range of α_p is narrower. The possible minimum α_p in the HER is somewhat larger than the required value.

From a chromaticity correction view point, the arc lattice built with π cells has a disadvantage in that the high peaks of η_x appear only in the phase steps of $N\pi$. This means that if we place sextupole pairs (SF's) for horizontal corrections only near the η_x peaks, corrections at the $(N + 1/2)\pi$ phases become difficult. Even if we add SF's at small η_x points, it is still less effective for $(N + 1/2)\pi$ phases than in the FODO case. As a result, the longitudinal dynamic aperture of the LER is unsatisfactory for the Touschek lifetime.

6.2.4 Noninterleaved 2.5π Cell

The 2.5π cell is created by combining five $\pi/2$ FODO cells and by merging ten bending magnets into four. In this cell structure, the bend magnets are arranged to form two dispersion bumps, so that we can keep small η_x at the dipole magnets, similar to the π cell case. By adjusting the positions of the bend magnets and η_x there, we can achieve the required emittance and momentum compaction factor at the same time for both rings. This flexibility of the 2.5π cell results in another merit for the HER: the existing bending magnets become re-usable in the HER arc, satisfying the requirements of the optics. Successive SF (SD) pairs in the 2.5π cell structure have a relative phase of $3\pi/2$. Thus, chromatic kicks at the $N\pi$ and $(N+1/2)\pi$ phases in both the horizontal and vertical planes can be corrected efficiently. The dynamic aperture of the 2.5π cell is significantly improved over previous schemes, and it satisfies all of the beam dynamics requirements. As shown in Figure 6.5, some higher-order chromaticity still remains, because the sextupole magnets are not sufficiently close to the main chromaticity sources in the interaction region. For this, further improvements can be achieved by a "localized chromaticity correction" in the interaction region, which is discussed in Section 6.2.5.

6.2.5 Noninterleaved 2.5π Cell with Local Chromaticity Correction

The local chromaticity correction refers to a scheme in which the large chromaticity produced by the final quadrupole magnets is corrected within the interaction region. Its advantage is that the creation of higher-order chromaticity can be avoided, by placing

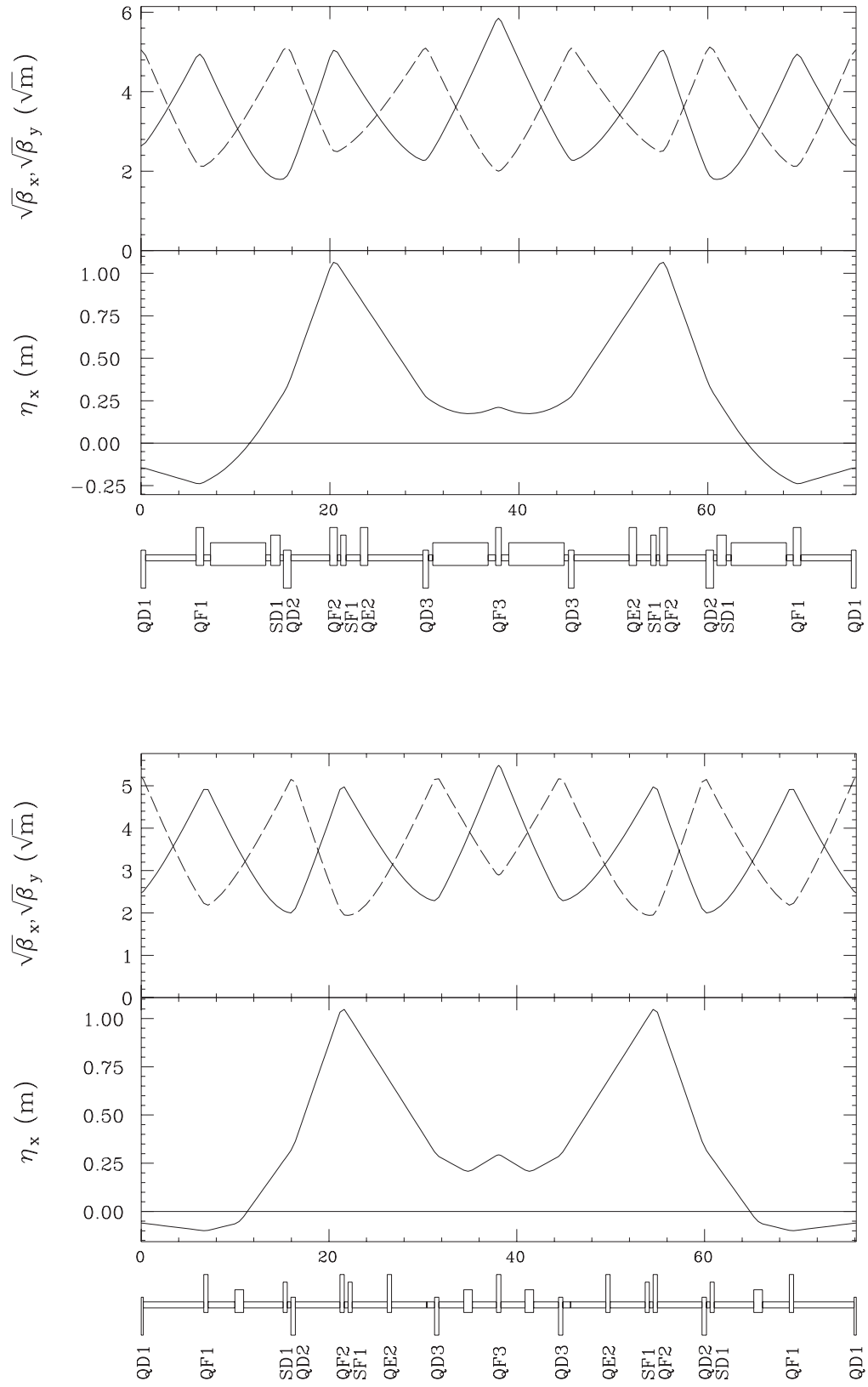

Figure 6.3: Structure of the 2.5π cell for the HER (above) and the LER (below).

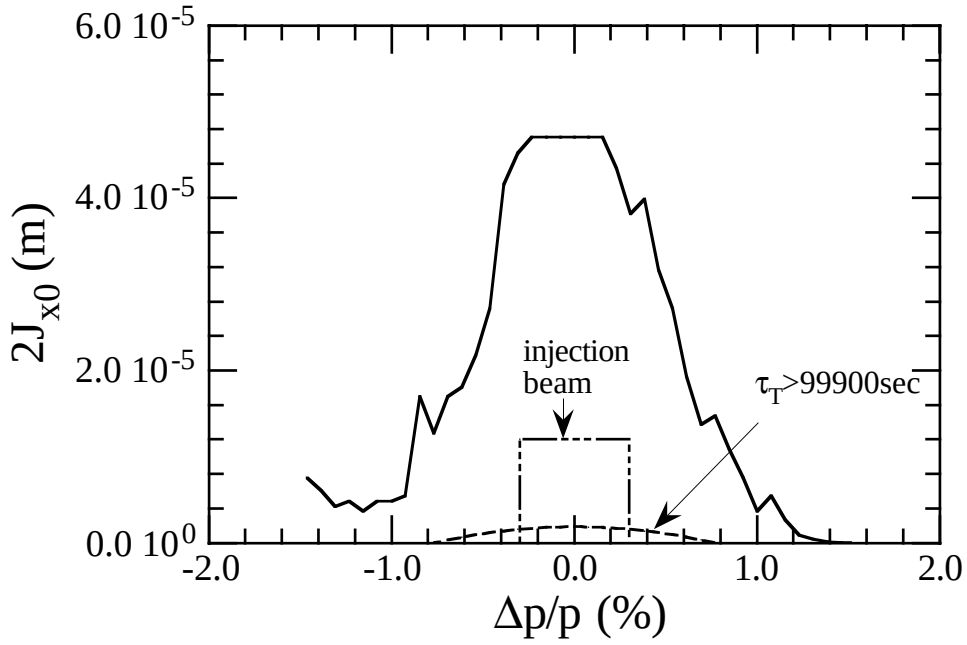

Figure 6.4: Dynamic aperture of the HER with the 2.5π cell.

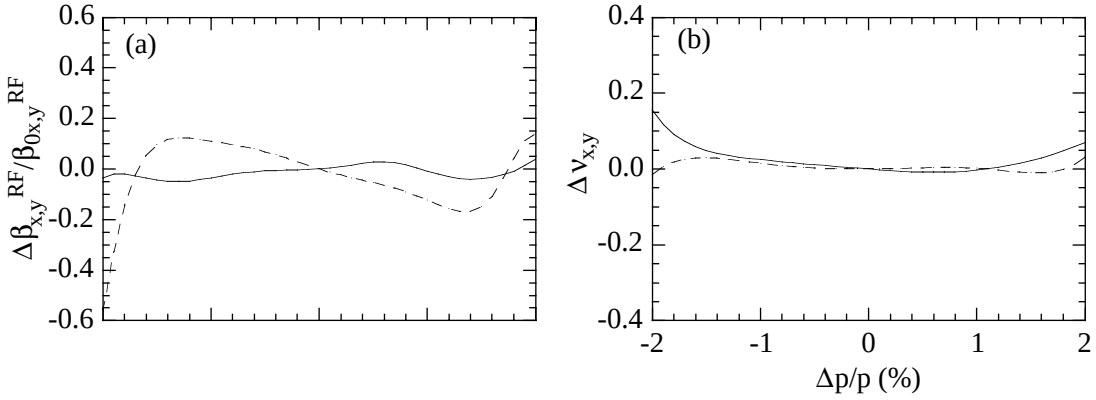

Figure 6.5: Chromaticity correction with the 2.5π cell for the LER.

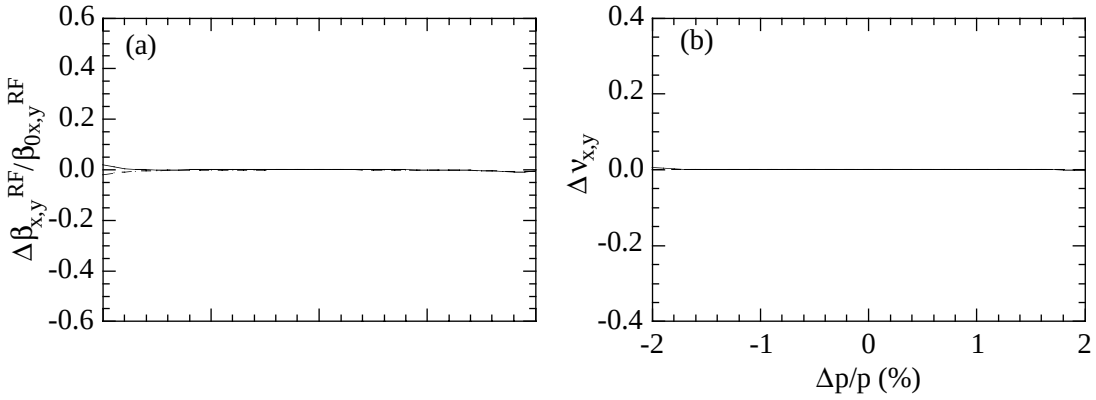

Figure 6.6: Chromaticity correction with the 2.5π cell and the local chromaticity correction for the LER.

sextupole magnets optically close to the final quadrupole magnets.

Pairs of vertical correction sextupole magnets are connected by the "pseudo $-I$" transformer, which is discussed in Section 6.2.6. Such sextupole pairs are placed in phase with the final quadrupole magnets near the IP. For those sextupole magnets, dispersive regions with large β_y/β_x ratios are created by adding bend magnets in the straight section. It is practically difficult to install two sextupole pairs for correcting both the horizontal and vertical planes in the IP straight section. Fortunately, the sources of the horizontal chromaticity are not so strongly localized as the vertical (*i.e.* a sizable amount of horizontal chromaticity comes from the arc and elsewhere, besides the final focusing section). Thus, we will place only one sextupole pair for the vertical correction in the straight section in each side of the IP. The last sextupole pairs (the pairs closest to the IP) at the end of the arc are used for the horizontal correction.

The design of the local chromaticity correction optics was done by minimizing the momentum dependence of optical parameters in a bandwidth of $2 \sim 3\%$. The optimum drift space length, and excitations of the quadrupole and sextupole magnets have been found. The local correction has significantly improved the chromaticity correction, as shown in Figure 6.6. Also, it has drastically improved the dynamic aperture in the region of large momentum deviations, resulting in a factor 1.5∼2 improvement of the Touschek lifetime over the optics without a local correction.

A local chromaticity correction scheme is considered for the LER to maximize the available dynamic aperture. Since the dynamic aperture requirement on the HER is less demanding, a local chromaticity correction will not be to implemented in HER.

6.2.6 Tunability of Beam Emittance and Momentum Compaction Factor with the Noninterleaved 2.5π Cell

It has been found that the 2.5π cell structure has a nice tunability feature, which allows us to adjust the beam emittance and momentum compaction. It is illustrated as follows. A noninterleaved sextupole pair in a 2.5π cell is connected with the transfer matrix,

$$\begin{pmatrix} -1 & 0 & 0 & 0 \\ m_{21} & -1 & 0 & 0 \\ 0 & 0 & -1 & 0 \\ 0 & 0 & m_{43} & -1 \end{pmatrix} . \tag{6.3}$$

Even if m_{21} and m_{43} are non-zero, nonlinear kicks by sextupole magnets are basically canceled within a pair. We have confirmed that this pseudo $-I$ transformer brings about a large dynamic aperture, comparable to a perfect $-I$. Then, by allowing $m_{21} \neq$

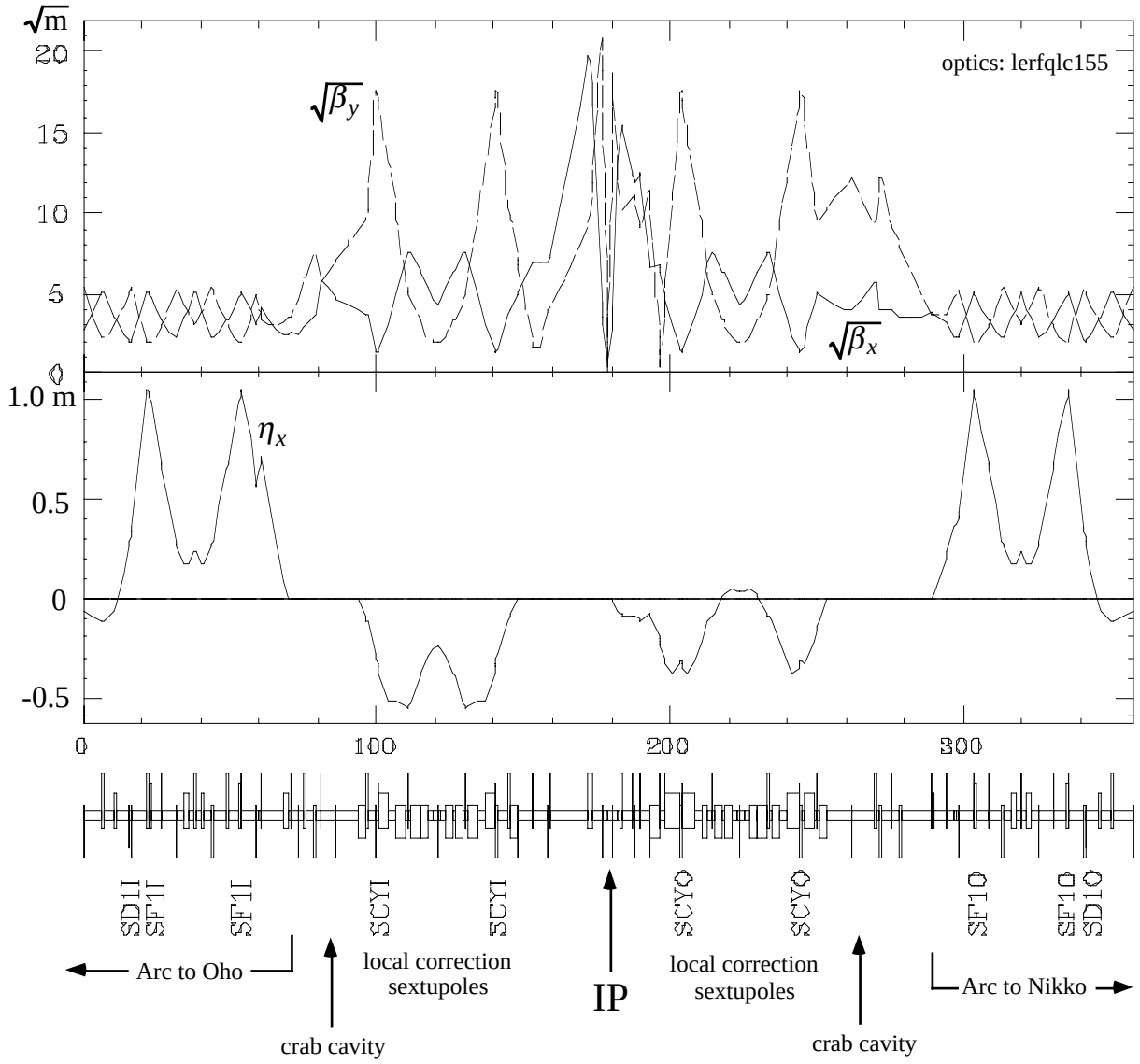

Figure 6.7: Optics of the local chromaticity correction for the LER. A pair of sextupole magnets for the vertical chromaticity correction is placed at each side of the IP.

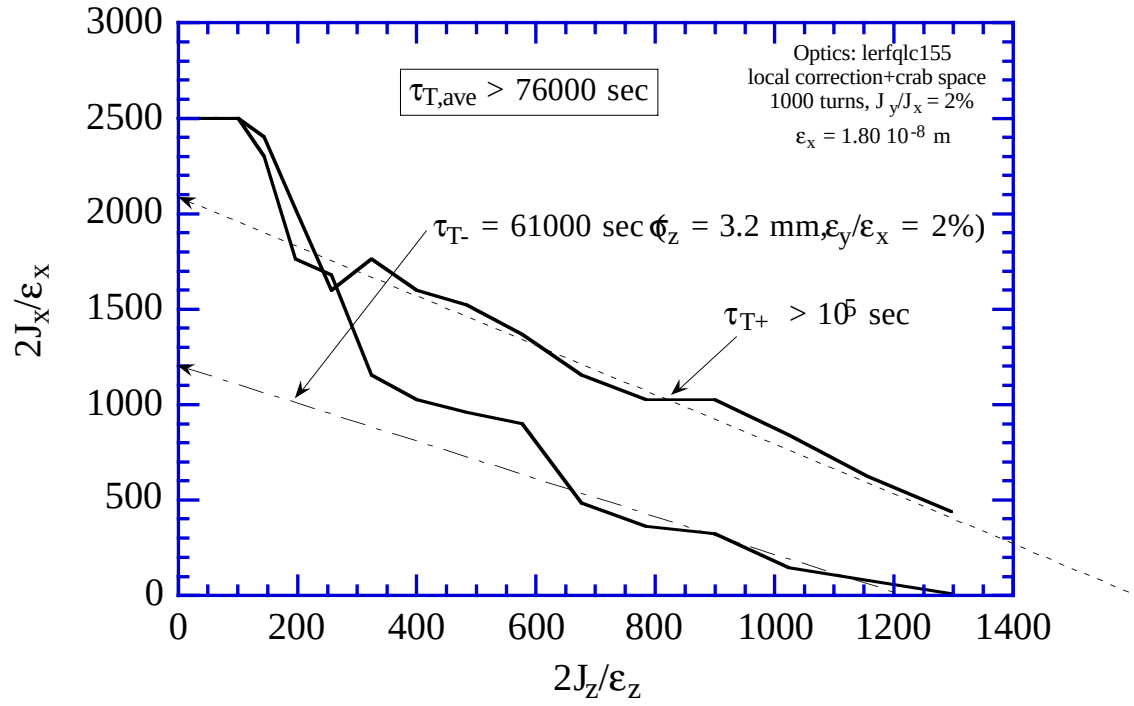

Figure 6.8: Dynamic aperture and Touschek lifetime of the LER with a local chromaticity correction.

0 and $m_{43} \neq 0$, two new free parameters become available for tuning. The "knobs" corresponding to these parameters may be the excitations of two families of quadrupole magnets (QF2 and QD2) outside the sextupole pairs. This allows us to tune α_p without breaking down the pseudo $-I$ transformation.

In the present design, the momentum compaction can be changed over the range of $-1 \times 10^{-4} \leq \alpha_p \leq 4 \times 10^{-4}$ by changing the strength of QF2's and QD2's by a few percent. During this time, ε_x is kept nearly constant. In practice, it is rather difficult to change ε_x over a wide range by only adjusting the two families of quadrupole magnets.

A cure to this restriction is to introduce a new family of quadrupole magnets QE2 inside the SF pair. By adjusting η_x at bend magnets, using five free parameters (QF2, QF3, QD2, QD3, and QE2), we can obtain the required tunability, $1.0 \times 10^{-8}\text{m} \leq \varepsilon_x \leq 3.6 \times 10^{-8}\text{m}$, while keeping α_p constant and maintaining the pseudo $-I$ condition between the SF's. In summary, a solution exists to tune ε_x and α_p independently by adding QE2's.

6.3 Optics Design of the Interaction Region

6.3.1 Compensation of the Detector Solenoid Field

One of the important issues in designing the optics around the IP is compensation of the x-y coupling effects generated by the detector solenoid field. Due to the finite crossing angle at the IP, the design beam orbits are not parallel to the detector solenoid axis. Thus, dispersion is also generated by the solenoid. Corrections have to be made for four coupling elements of the transfer matrix between the IP and the arc, as well as the dispersion near the IP.

A possible solution to this is to add four or more skew quadrupole magnets and several bend magnets at each side of the IP. This correction, however, is perfect only for on-momentum particles. The chromaticity of the x-y coupling remains uncorrected, and can significantly increase the "anomalous emittance" at

$$\begin{aligned} \nu_x \pm \nu_y \pm m\nu_s &= N \\ 2\nu_{x,y} \pm m\nu_s &= N \ . \end{aligned} \tag{6.4}$$

The use of skew quadrupole corrections reduces the dynamic aperture, as shown in Figure 6.10.

The best way to compensate for the x-y coupling effects of the detector solenoid is to use counter solenoids, so that the integrated field, $\int B_z ds$, becomes zero within the drift space around the IP. This compensation works perfectly for particles with any momentum. This is the solution that has been adopted in the design of KEKB.

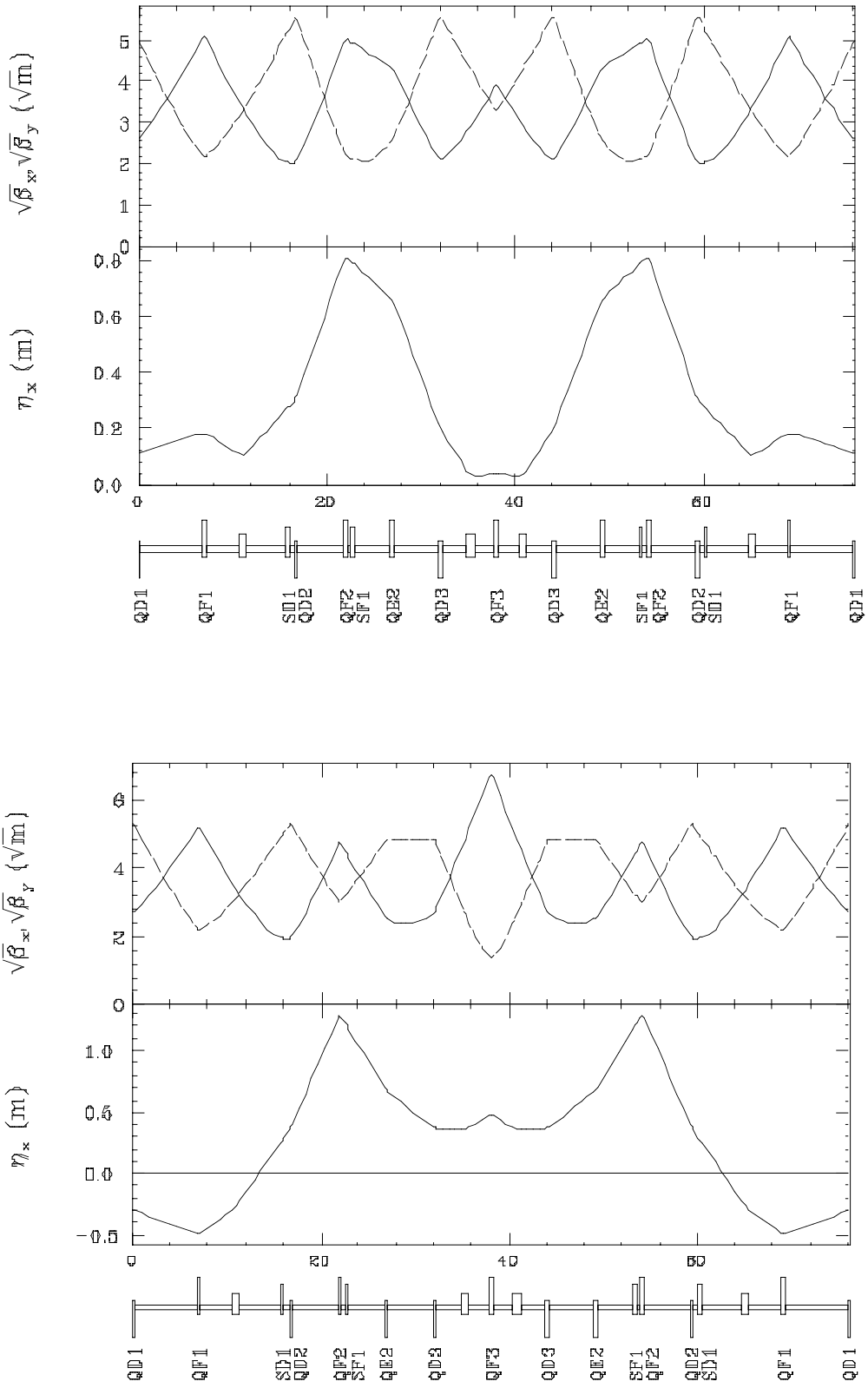

Figure 6.9: Examples of emittance control in the LER: $\epsilon_x = 1.0 \times 10^{-8}$m (above) and 3.6×10^{-8}m (below).

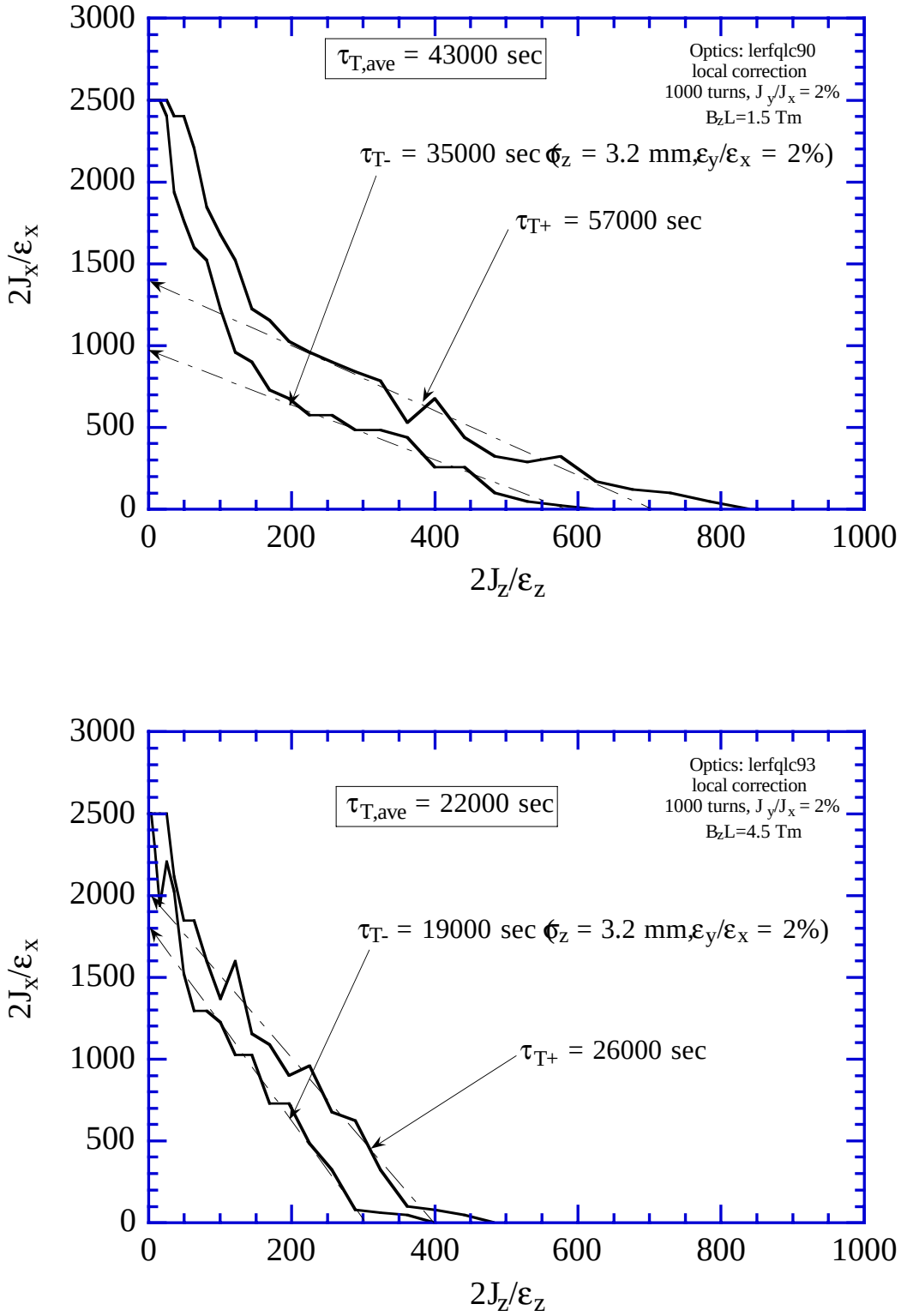

Figure 6.10: Dynamic aperture of the LER with an integrated solenoid field of 1.5 Tm (above) and 4.5 Tm (below).

6.3.2 Crab Cavities

An optional use of a crab crossing scheme is currently being studied. To minimize the required number of crab cavities, the transverse kicks given by the cavities should have a maximum effect on the bunch orientation at the IP. This means that the horizontal phase distance of the crab cavities from the IP should be $(N + 1/2)\pi$. From the lattice design view point, it is possible to reserve such a dispersion-free drift space in the straight section near the arc.

The dynamic aperture has also been checked with the crab cavities. It has been shown that the dynamic aperture is quite insensitive to the crab cavities, even with a large amount of errors in the amplitudes and phases of the crab-mode RF kicks.

6.4 Optics Design of Other Straight Sections

This area of the design is still in progress. The following issues will be discussed in a future version of the design report.

- Dispersion suppressors:
- Symmetry points of arcs:
- Optics with wigglers: As discussed in Chapter 2, the parameter sets for the HER and the LER are almost identical. However, if the radiation loss is assumed to come only from bend magnets in the arcs, the radiation damping time of the LER is longer than that of the HER by a factor of 2. To halve the LER damping time, without increasing the momentum spread, preparation is under way to install optional damping wigglers for a total length of 96 m in Oho and Nikko. These wigglers can be also used to control the LER beam emittance. We can obtain the required tunability of the horizontal emittance by the wigglers.
- Adjustment of the path length: Changes of the path length due to the wigglers can be adjusted by special sections called "chicanes". Each section is built with four bending magnets, which are placed in a way similar to that of a unit of wigglers. The LER has four 12 m-long chicanes, which provide a sufficient tunability of the path length. These chicanes can also be used to equalize the circumference of the LER to that of the HER. Figure 6.11 shows the optics design of the LER in the vicinity of the chicane structure. The chicane bend magnets are labelled BC1 and BC2 in Figure 6.11.
- Injection point:

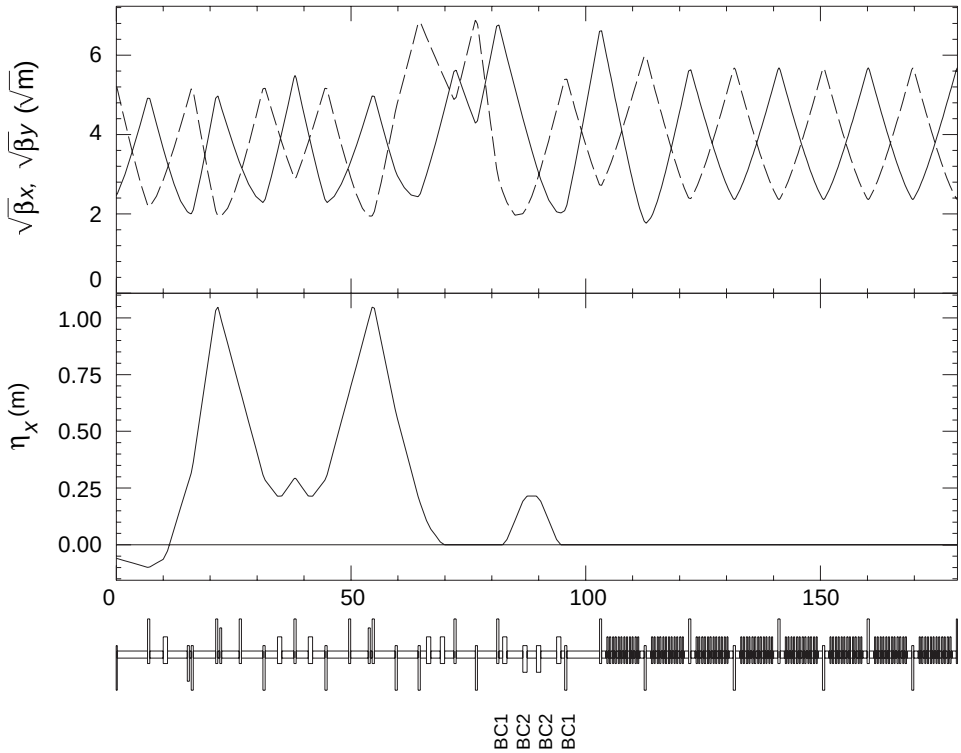

Figure 6.11: Optics design of the LER in the vicinity of the chicane structure for ring length adjustments. The chicane bend magnets are labelled as BC1 and BC2.

- Translation chicane:

6.5 Requirements on the Magnet Quality

The tolerances on the systematic multipole errors of the bend magnets and quadrupole magnets in the arcs have been estimated. The criteria is based on a 2% reduction of the dynamic aperture integrated in both the momentum and transverse phase spaces. The results are listed in Table 6.2. In the table K_n is defined as

$$K_n = \frac{1}{B\rho}\frac{\partial^n B_y}{\partial x^n}. \tag{6.5}$$

It is known that requirements similar to those listed in Table 6.2 have been met by existing magnets that are used for the TRISTAN main ring.

		$\Delta B/B$ at 50 mm radius
Dipole Magnets		
K_2/K_0	1.0m^{-2}	0.12%
K_4/K_0	17000m^{-4}	0.45%
Quadrupole Magnets		
K_5/K_1	22000m^{-4}	0.12%
K_9/K_1	$1.3 \times 10^{13}\text{m}^{-8}$	0.45%

Table 6.2: Tolerances of systematic multipole errors.

6.6 Effects of Machine Errors and Tuning Procedures

The performance of the noninterleaved scheme lattice may be sensitive to machine construction errors, which break down the cancellation of sextupole aberrations in the $-I$ transformation. This section considers the effects of the construction and setup errors in the ring lattice, and their tolerances for the acceptable operation of KEKB. The criteria used in this analysis are the emittance ratio, the dynamic aperture, and the miss-crossing at the IP. The errors considered include: the misalignment of magnets, BPM offset and field ripple.

Concerning magnet misalignment, we consider the combined effect of temperature-dependent drift, movement of the tunnel, vibration of the magnets and others. No attempts are being made to resolve individual errors, or to quote their tolerances separately. This is because there is no sufficient information available for fixing their relative contributions at this stage.

In this section the tolerances are *not* discussed in the form of the maximum allowable errors, which may be considered to be the common definition. Rather, we assume certain combinations of initial lattice errors, and simulate how the emittance ratio and dynamic aperture can be improved by applying a series of beam-based tuning procedures. This study has been performed by using a sophisticated beam simulation code SAD, which has been developed at KEK. In this study an analysis was made on what magnitude of combined errors are still acceptable, such that the target emittance ratio and the dynamic aperture, etc. can be achieved by realistic beam-based tuning. This approach clarifies the significance of each tuning process and its role. It also helps to create guidelines for the development of beam-based techniques of error analyses.

The errors used in the simulation are given in Table 6.3. The assumptions used in

Element	Δx(mm)	Δy(mm)	$\Delta\theta$(mrad)	Δk/k
Quadrupole Magnets	0.15	0.15	0.2	$1 \times 10^{-}3$
QC Quads[2)]	0.01	0.01	0.1	$1 \times 10^{-}4$
Sextupole Magnets	0.15	0.15	0.2	$2 \times 10^{-}3$
Bend Dipole Magnets		0.1	0.1	$2 \times 10^{-}3$
Steering Corrector Magnets		0.1	0.2	
BPMs[3)]	0.075	0.075		

[1)]The values are for one standard deviation (σ).

[2)] Two quads near IP(QCS and QC1).

[3)] Assume Beam-based measurement of BPM offset.

Table 6.3: Errors used in the simulation[1)]

the simulation are summarized as follows:

1. Only the LER has been considered. The situation at HER is expected to be similar, since its arc lattice structure is basically identical to that of the LER.

2. Errors of the quadrupole magnets close to the interaction point (QCS and QC1) are intentionally assumed to be very small compared to those in the arc section. This is done in order to magnify the effects of the errors in the arc section. We will consider the effects of QCS and QC1 separately in the near future.

3. Every sextupole magnet has a mover which can transversely move the magnet with a maximum stroke of ± 3 mm in both the horizontal and vertical directions.

4. The offset errors of the BPMs relative to the magnetic center of the quadrupole and sextupole magnets are assumed to be measurable with an accuracy of 75 μm. This is considered to be achievable, for example, by using the K-modulation method [4, 5].

5. The strength errors of the quadrupole magnets are assumed to be measurable with an accuracy of 0.1%. The measurement may be directly performed prior to installation, or by using beam orbit bumps across each magnet.

6. The errors are assumed to obey Gaussian distributions with a cut-off at 3 standard deviations (3σ). Their magnitudes are given in Table 6.3.

6.6.1 Emittance ratio and Dynamic aperture

Simulations with 20 different random seeds (events) have been conducted. Figure 6.12 shows the machine performance at various stages of beam tuning. The graphs show the emittance ratio plotted against β_y (m) at the interaction point, and the estimated dynamic aperture ($n_x \equiv \sqrt{2J_x/\epsilon_{x_0}}$ vs. dp/p). The operation point was set to be (ν_x,ν_y)=(46.52, 46.08), which is preferred from the viewpoint of beam-beam effects (see Chapter 3).

In the tracking calculation, the initial vertical amplitude was set to be one third that of the horizontal. In the plots for the emittance ratio, the black dots represent results from individual "events" that correspond to different random seeds for errors. The straight broken line indicates the design emittance ratio of 2%. In the dynamic aperture plots, the thick lines indicate the expected dynamic aperture in the error-free lattice, while the thin lines show the results from simulations with random lattice errors. The injected beam is expected to occupy the area indicated by the thick rectangle.

Plots (a1) and (a2) are for only orbit corrections, while (b1) and (b2) are for sextupole adjustments by movers, in addition to orbit corrections.

It can be seen that for the "orbit correction only" case, the emittance ratio is huge, and the dynamic aperture (DA) is degraded compared to the "error-free" case (thick line). Although the DA has sufficient space to accept the injected beam, it is desirable to have much more margins for safety, especially for large momenta, because it limits the Touschek lifetime.

In order to improve the emittance coupling, sextupole magnets are vertically moved, simulating movers, such that the orbit passes through their center within 75 μm. The emittance ratio is dramatically improved, as shown in (b1). The corresponding DA also shows a small improvement for the transverse direction.

The scatter of β_y^* in (a1) and (b1) is fairly large ($\sim \pm 25\%$). This is a reflection of strength errors of the quadrupole magnets that are included in the simulation. It has been found that DA is strongly correlated with β_y^*. Thus although those "events" with smaller β_y^* give a larger luminosity, they are also responsible in part for the deteriorated DA in (b2).

In the next simulation step optics matching was performed, assuming that the strength errors of the quadrupole magnets are known with an accuracy of 0.1%. This has the effect of making the expected β_y^* of each "event" closer to the design value. As shown in (c1), the spread of β_y^* is much reduced. However, as shown in (c2), DA becomes much worse for large momenta. This is because the strengths of the sextupole magnets are no longer optimum for the re-matched optics.

As the final step, by optimizing the sextupole magnets we could recover the DA

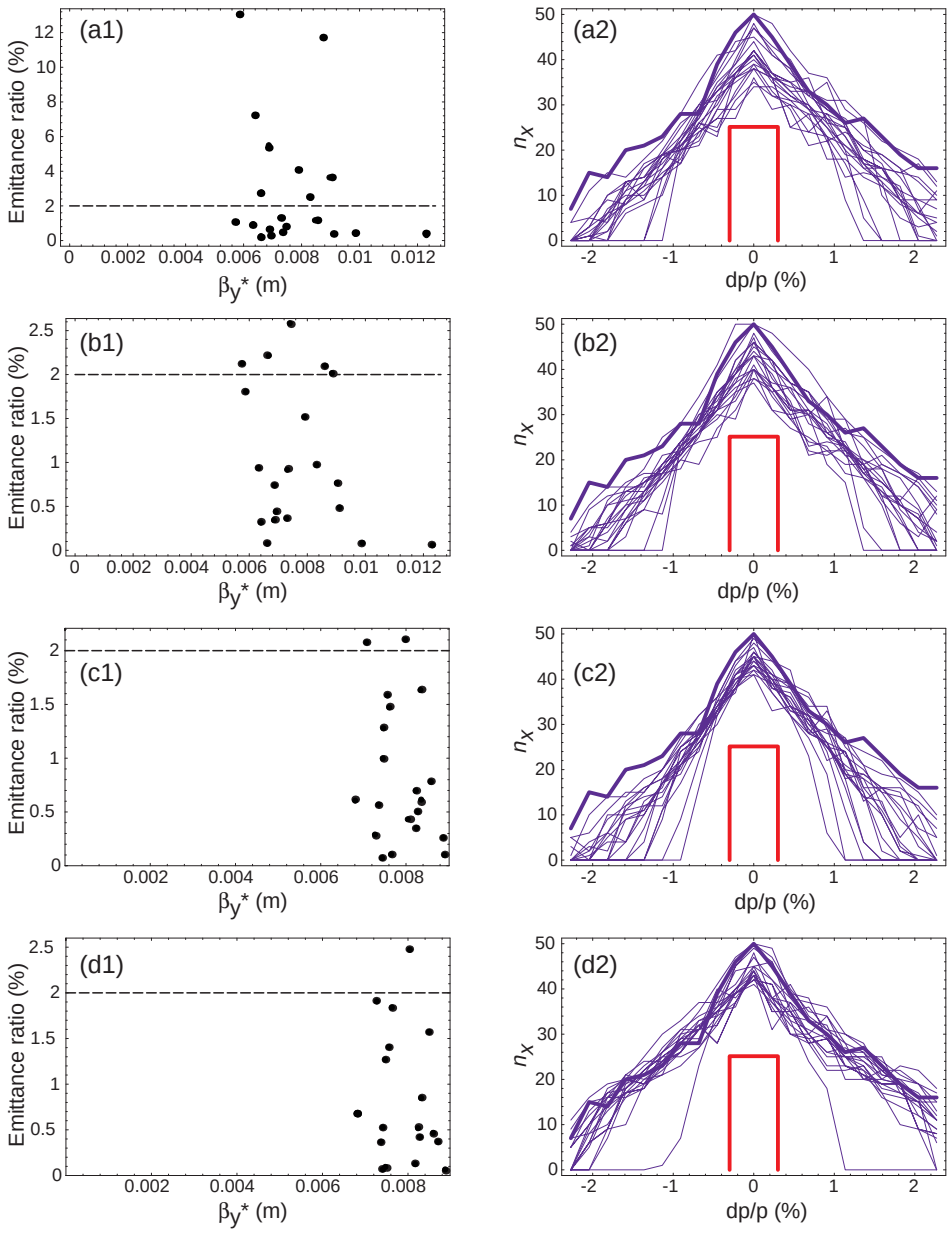

Figure 6.12: Simulated machine performance at various stages of beam tuning. The graphs show the emittance ratio plotted against β_y (m) at the interaction point, and the estimated dynamic aperture ($n_x \equiv (2J_x/\epsilon_{x_0})^{-1/2}$ vs. dp/p). Plots (a1) and (a2) are for only orbit corrections, while (b1) and (b2) are for sextupole adjustments by movers, in addition to the orbit corrections. Plots (c1) and (c2) show the case with optics re-matching. Plots (d1) and (d2) show the results with chromaticity correction for re-matched optics. For detailed descriptions see the text.

close to the ideal, as shown in (d1) and (d2). (There was one exception for which we could not find the optimum setting of the sextupole magnets).

It can be seen that tuning with sextupole mover is very effective to optimize the emittance coupling, because it is orthogonal to the DA: it does not affect the dynamic aperture.

6.6.2 Field Ripples

If the excitation strengths of the magnets change at frequencies for which the orbit feedback system cannot apply corrections effectively, then noticeable performance degradation may result. To evaluate this issue, the tolerances on the field jitter of the magnets have been calculated.

The criteria for calculating the jitter tolerances are that: (1) changes in the field do not induce either emittance growth or a deterioration of DA by more than 10%, and (2) shifts of the beam orbit at the IP do not exceed $0.1\sigma^*_{x,y}$.

The calculated tolerances of the field jitter are summarized in Table 6.4. The tolerances on the sextupole jitters are smaller than those for the quadrupole magnets. The QCS quadrupole magnets for the final focusing are assumed to be connected in series to a common power supply. The third column in the table gives the effect of jitter on the emittance or DA. The symbols Δx^* and Δy^* are the horizontal and vertical orbit deviations at the IP. The ratio $\Delta A/A_0$ is the relative change in the area of the dynamic aperture, *i.e.*, the sum of n_x for each dp/p point.

It should be noted that the tolerances quoted in the table are for the field, and that the numbers are not to be considered directly for the magnet power supply. To estimate the tolerances on the ripples of the magnet power-supplies, the effects of eddy currents in the vacuum chamber have to be taken into consideration. Generally, the power-supply ripple tolerances are much more relaxed than the values shown in Table 6.4. For example, the tolerances of the 50 Hz component of the power supply ripples are 10 times greater than those given in Table 6.4

6.7 Conclusions

Detailed studies on the lattice for the arc sections of KEKB have been performed. The present working design is based on a 2.5π cell structure. It offers an excellent dynamic aperture, and tunability of momentum compaction and beam emittance. The use of a local chromaticity correction scheme near the IP appears to be very promising. The requirements on the magnet field quality and errors of alignment and magnet excitations have been studied.

Element	relative jitter (σ)	what limits
Bend Dipole Magnets	1×10^{-5}	$\Delta x^* = 3.4\mu$m ($\sigma_x^* = 80\mu$m)
Quadrupole Magnets	1×10^{-4}	$\epsilon_y/\epsilon_{y_0} = 5 \pm 19\%$ $\Delta A/A_0 = -3 \pm 14\%$
QCS Quads	1×10^{-5}	$\epsilon_y/\epsilon_{y_0} = 10\%$ $\Delta A/A_0 = -10\%$
Sextupole Magnets		
Steering Corrector Magnets	1×10^{-5}	$\Delta y^* = 0.1\mu$m ($\sigma_y^* = 2\mu$m)

Table 6.4: Tolerances of field jitter. Symbols Δx^* and Δy^* denote the horizontal and vertical orbit deviations at the IP, while the $\Delta A/A_0$ is the relative change of the area of the dynamic aperture plot, *i.e.*, the sum of n_x for each dp/p point.

Bibliography

[1] K.L. Brown, IEEE Trans. Nucl. Sci. **NS-26**, 3490 (1979); K.L. Brown and R. Servranckx, in *Physics of High Energy Particle Accelerators*, Proc. the Third Annual U.S. Summer School in High Energy Particle Accelerators, AIP Conf. Proc. No. 127 (1983).

[2] K. Oide and H. Koiso, Phys. Rev. **E47**, 2010 (1993).

[3] K. Oide and H. Koiso, Phys. Rev. **E49**, 4474 (1994).

[4] R. Schmidt, *Misalignments from K-modulation*, Proceedings of The Third Workshop on LEP Performance, Chamonix, January, 1993, 139-145

[5] M. Kikuchi, K. Egawa, H. Fukuma and M. Tejima *Beam-Based Alignment of Sextupoles with Modulation Method*, to be published